Journal of Agrometeorology

(A publication of Association of Agrometeorologists)

ISSN : 0972-1665 (print), 2583-2980 (online)

Vol. No. 28 (3) :324-335 (September - 2026)

https://doi.org/10.54386/jam.v28i3.3274

https://journal.agrimetassociation.org/index.php/jam

Research paper

Monitoring Wheat Vegetation Health and Moisture-Related Spectral Variation Using Landsat 8-Derived Indices in Punjab

GURLEEN KAUR[1], SREETHU S.[1], VIKAS SHARMA[*2] and VANDNA CHHABRA[1]

[1]*Department of Agronomy, School of Agriculture, Lovely Professional University, Phagwara, Punjab, India*

[2]*Department of Soil Science and Agricultural Chemistry, School of Agriculture, Lovely Professional University, Phagwara, Punjab, India*

[*]*Corresponding Author email: vikas.27227@lpu.co.in*

ABSTRACT

Efficient monitoring of wheat growth and moisture-related stress is critical for improving irrigation management in Punjab, where groundwater depletion and climate variability threaten crop productivity. This study used Landsat 8 Surface Reflectance data processed in Google Earth Engine to assess vegetation health, phenological dynamics, and moisture-related spectral variation during the *rabi* seasons of 2022–23 and 2023–24 in Phagwara, Punjab. The Normalized Difference Vegetation Index (NDVI), Land Surface Water Index (LSWI), and False Colour Composite (FCC) were analysed at regional and selected field scales. FCC imagery clearly captured seasonal changes in vegetation cover and crop development. NDVI showed a consistent wheat growth pattern, increasing from sowing and early establishment to peak vegetative–reproductive stages, followed by decline during maturity due to senescence and canopy drying. Field-level NDVI trends corresponded well with observed phenological stages and crop growth indicators, including plant height, leaf area index, and relative water content under contrasting irrigation conditions. NDVI-based classification further distinguished wheat and non-wheat pixels within the selected study area. LSWI provided supplementary information on moisture-related spectral variation associated with rainfall, crop stage, and canopy condition. Overall, the integrated use of NDVI, FCC, and LSWI provides a practical framework for monitoring wheat growth and supporting irrigation decision-making.

Keywords: Soil moisture stress; Wheat phenology, NDVI; LSWI; Landsat 8; Remote sensing

Punjab, Haryana, and Uttar Pradesh together contribute nearly 80% of India's wheat production**,** with Punjab alone cultivating about 3.52 million hectares**,** producing 14.82 million tonnes of wheat at a productivity of 4.206 t ha^{-1} (Government of India, 2022). Punjab has played a vital role in ensuring national food security; however, groundwater overexploitation and land degradation now threaten its agricultural sustainability (Kaur *et al.,* 2010; John & Babu, 2021). Inefficient canal irrigation and subsidized electricity have driven groundwater extraction beyond sustainable limits—by nearly 72% (Srivastava *et al.,* 2015; Sidhu & Chopra, 2022). Efficient irrigation scheduling has therefore become essential to sustain wheat productivity under limited water availability. Climate variability, particularly rising temperatures and erratic rainfall, has further aggravated heat and moisture stress in wheat-growing regions. A 1°C rise in temperature may reduce global wheat yield by about 6% due to heat-induced physiological stress (Shi *et al.,* 2022). Since soil moisture strongly influences photosynthesis, chlorophyll content, and canopy development, monitoring crop growth and moisture-related indicators is crucial for optimizing water use and maintaining crop health. Conventional field-based approaches for assessing soil and plant water status are accurate but spatially restrictive and labour-intensive. Advances in remote sensing technology have enabled the large-scale, non-destructive assessment of vegetation and soil moisture dynamics with high temporal and spatial resolution. Among various remote sensing metrics, the Normalized Difference Vegetation Index (NDVI)**,** Land Surface Water Index (LSWI)**,** and False Colour Composite (FCC) are widely recognized for their ability to evaluate vegetation vigour, canopy moisture, and surface conditions. The NDVI**,** derived from red and near-infrared (NIR) reflectance, provides a reliable measure of vegetation greenness and photosynthetic activity (Yang *et al.,* 2010; Radočaj *et al.,* 2023). The LSWI, which combines

Article info - DOI: *https://doi.org/10.54386/jam.v28i3.3274*

Received:26 November 2025; Accepted: 18 June 2026; Published online : 7 September 2026

NIR and shortwave infrared (SWIR) reflectance, is sensitive to moisture-related spectral variation in soil and vegetation canopies and can provide supplementary information on crop water-related conditions. The FCC generated using NIR, red, and green bands, visually enhances the distinction between vegetation, built-up areas, and water bodies, aiding intuitive interpretation of spatial moisture stress and vegetation health. The integration of NDVI, LSWI, and FCC provides a useful framework for monitoring wheat vegetation health, phenological development, and moisture-related spectral variation across temporal scales. This study evaluates wheat crop growth and moisture-related dynamics using Landsat 8-derived spectral indices, namely NDVI, LSWI, and FCC, over two consecutive *Rabi* seasons, 2022–23 and 2023–24, in the Phagwara region of Punjab. Such approaches are especially valuable in regions like Punjab, where farmers face increasing challenges in managing water resources efficiently. The objective of this study was to develop a multi-temporal remote sensing framework for assessing wheat vegetation health, phenological dynamics, and moisture-related spectral variation in Punjab using Landsat 8 imagery. Specifically, the study aimed to: (i) analyse spatio-temporal variation in wheat vegetation vigour using NDVI; (ii) compare regional and selected field-level NDVI responses across two *rabi* seasons; (iii) identify wheat and non-wheat pixels within the selected study area using NDVI-based classification; (iv) relate temporal NDVI trends with field-observed wheat phenological stages and crop growth observations; and (v) interpret LSWI as a supplementary indicator of moisture-related spectral variation in relation to crop growth stages, rainfall distribution, and field-observed crop water status.

MATERIAL AND METHODS

Study area: The study was conducted in the Phagwara region, Punjab, India (31.22° N, 75.77° E), with experimental trials carried out at the LPU Research Farm, Lovely Professional University, Phagwara (Fig. 1). The farm represents typical rabi-season agricultural conditions of the region, with alluvial soils and a subtropical climate characterized by low rainfall and cooler temperatures during November to April. The experimental plots were used to monitor crop growth, vegetation health, and water stress under standard agronomic practices. Meteorological data for the 2022–23 (Fig. 2a) and 2023–24 (Fig. 2b) *rabi* seasons indicated notable seasonal variation during wheat growth. The temperature ranged from 7.3 to 36.5 °C in 2022–23 and from 4.64 to 34.66 °C in 2023–24, while total rainfall was 118.5 and 104.5 mm, respectively.

Field observations and ground reference data

Field observations were recorded from wheat experimental plots at the LPU Research Farm during the *rabi* seasons of 2022–23 and 2023–24. The experiment included different irrigation scheduling treatments, namely recommended irrigation, irrigation at critical growth stages, plant stress index-based irrigation, field-capacity depletion-based irrigation, and rainfed conditions For field-level interpretation of satellite-derived spectral indices, selected field observations from the LPU experimental wheat field were used as ground reference data. Among the irrigation treatments, T_1 (recommended irrigation at growth stages such as CRI, Tillering, Booting, Heading and Anthesis) and T_2 (rainfed) were selected for comparison because they represented contrasting crop water conditions: T_1 reflected optimum irrigation and normal crop growth, whereas T_2 represented moisture-limited conditions. This contrast was used to support the interpretation of NDVI variation in relation to canopy development, LAI, plant height, and crop phenology, and to support the moisture-related interpretation of LSWI.

Leaf Area Index: Leaf area index (LAI) was recorded at 30, 60, 90, and 120 DAS. Representative plants were selected from each plot, and five fully expanded leaves per plant were used to measure leaf area with an automatic leaf area meter (Model 211, Systronics). Total leaf area per plant was estimated by multiplying the average leaf area by the total number of leaves per plant.

Relative Water Content (%): Leaf relative water content (RWC) was measured during 60, 90 and 120 DAS. Representative leaf samples were collected from each plot, and their fresh weight (FW) was recorded immediately after sampling. The leaves were then immersed in distilled water for 24 h to attain full turgidity, gently blotted to remove surface moisture, and weighed to obtain turgid weight (TW). Thereafter, samples were oven-dried at 60 °C until constant weight to determine dry weight (DW). RWC was calculated following Barrs & Weatherley (1962) using the formula:

$$\text{RWC (\%)} = \frac{\text{Fresh weight} - \text{Dry weight}}{\text{Turgid weight} - \text{Dry weight}} \times 100$$

Landsat 8 data acquisition and preprocessing

Landsat 8 Surface Reflectance data were used to derive NDVI, LSWI, and FCC maps for the *rabi* seasons of 2022–23 and 2023–24. Image processing was carried out in Google Earth Engine. The study area was delineated using a polygon boundary, and images with less than 10% cloud cover were selected (Table 1). Clouds and shadows were masked using the QA_PIXEL band. Monthly median composites were generated from available cloud-free images to reduce cloud contamination, atmospheric noise, and short-term image variability. Therefore, the monthly maps represent composite conditions for each month rather than a single image acquisition date.

False colour composite generation

False Colour Composite (FCC) images were generated using near-infrared, red, and green bands. In Landsat 8, Band 5 (NIR), Band 4 (red), and Band 3 (green) were assigned to the red, green, and blue channels, respectively. FCC images were used to visually interpret vegetation cover, crop growth conditions, soil exposure, built-up areas, and water bodies across the Phagwara region and the selected study area.

Normalised difference vegetation index (NDVI): It is a crucial vegetation index widely employed in global studies of climatic and environmental changes (Bhandari *et al.,* 2012). It is calculated using the ratio of canopy reflectance in the red (Band 4) and near-infrared (Band 5) bands (Nageswara *et al.,* 2005). It can be calculated using the formula given by Tucker, (1979).

$$NDVI = \frac{NIR - Red}{NIR + Red}$$

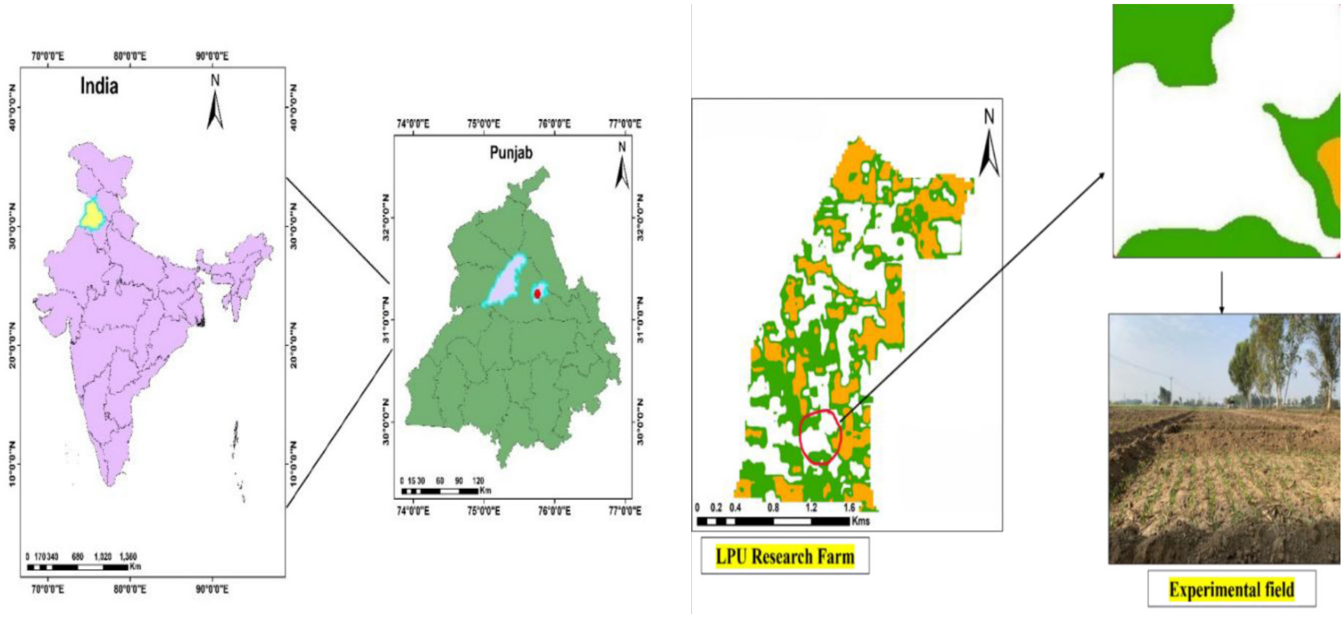

Fig. 1: Location of the study area in India and Punjab, showing the LPU Research Farm field boundary used for extracting Landsat 8-derived spectral indices and reflectance values

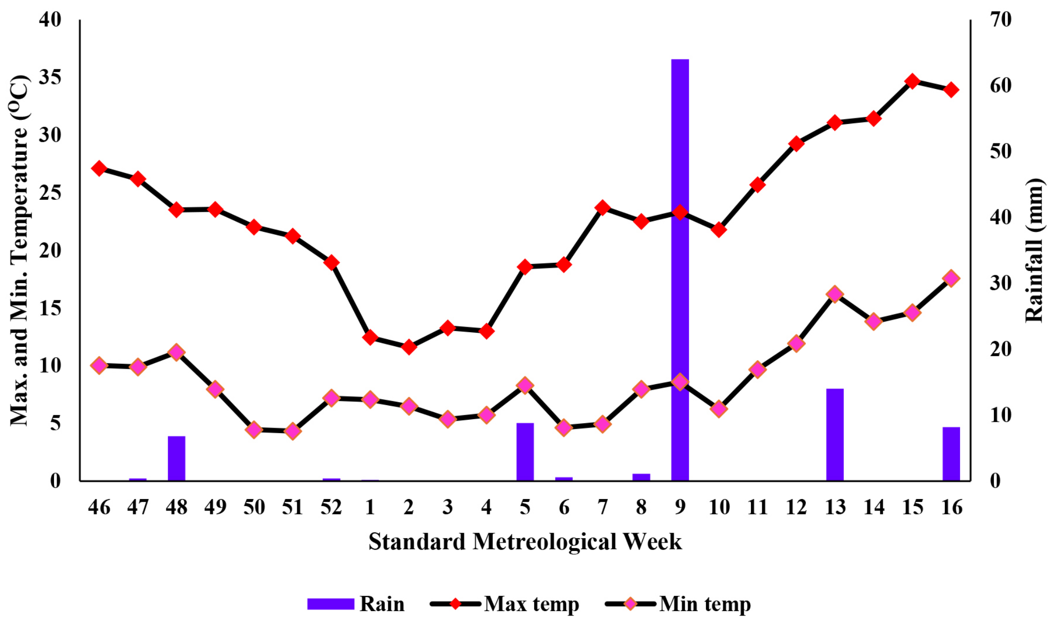

Fig. 2(a): Weekly metrological data recorded for crop season of 2022-23

Land surface water index (LSWI): Shortwave infrared (SWIR) (Band 6) and near-infrared (NIR) (Band 5) are used to calculate the land surface water index (LSWI). In the SWIR, liquid water absorbs a large amount of light, and the LSWI is sensitive to the overall water content in vegetation (Chandrasekar *et al.,* 2010).

$$LSWI = \frac{NIR - SWIR}{NIR + SWIR}$$

In the present study, LSWI was used as a supplementary moisture-related spectral indicator. Due to the unavailability of stage-wise mean LSWI values, direct statistical correlation between LSWI and field-measured relative water content could not be performed. Therefore, LSWI was interpreted cautiously in relation to crop growth stages, rainfall distribution, and field-observed moisture-related trends.

Temporal NDVI profile and phenological stage linkage

For temporal NDVI analysis, date-wise NDVI values were extracted from the selected LPU Research Farm boundary using Landsat 8 Surface Reflectance imagery in GEE. The extracted NDVI values were plotted against image acquisition dates to generate temporal NDVI profiles for wheat during the *rabi* seasons

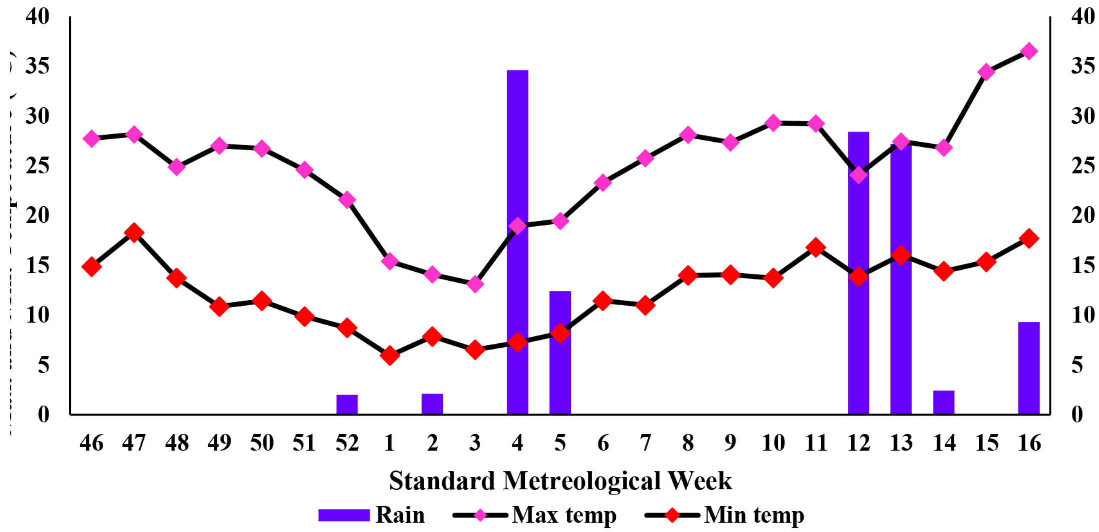

Fig. 2(b): Weekly metrological data recorded for crop season of 2023-24

Table 1: Landsat 8 bands used for NDVI, LSWI, FCC and spectral reflectance analysis

Index/Output	Landsat 8 bands used	Purpose
FCC	Band 5, Band 4, Band 3	Vegetation and land-cover visualization
NDVI	Band 5 and Band 4	Crop vigour and canopy greenness
LSWI	Band 5 and Band 6	Canopy/soil moisture indication
Spectral reflectance	Bands 2–7	Growth-stage-wise reflectance pattern

of 2022–23 and 2023–24. Field-observed phenological stages, including sowing, crown root initiation, tillering, booting, heading, anthesis, milking, dough, and maturity, were overlaid on the NDVI curves. This helped interpret whether changes in satellite-derived NDVI corresponded with actual wheat growth and phenological development.

Wheat pixel identification and classification

Wheat pixels were identified using a phenology-guided NDVI approach. Pixels showing the typical wheat growth trajectory—low NDVI during November due to sowing and early establishment, increasing NDVI during December to February due to canopy development, peak NDVI during February–March corresponding to heading and anthesis, and declining NDVI during April due to senescence and maturity-were classified as wheat.

Pixels that did not follow this temporal NDVI pattern were treated as non-wheat and excluded from wheat-specific analysis. FCC images were also used for visual confirmation of vegetation cover, while built-up areas, fallow land, water bodies, and non-crop vegetation were masked out.

Data analysis and map preparation

All image processing, index calculation, pixel extraction, and temporal analysis were performed in Google Earth Engine. The analysis was conducted at two spatial scales: the Phagwara regional scale and the selected LPU Research Farm field scale. Regional-scale maps were generated to show spatial variability in vegetation and moisture-related spectral patterns across the Phagwara region, whereas the selected field boundary was used for field-specific extraction of NDVI and LSWI values. The extracted NDVI values were used to generate temporal NDVI profiles and study-area-specific maps. Final NDVI, LSWI, FCC, and wheat/non-wheat classification maps were prepared using ArcGIS for interpretation and presentation.

RESULTS AND DISCUSSION

The FCC, NDVI, and LSWI maps are presented at both the regional (Phagwara) and research farm scales. The regional maps provide an overview of spatial variability in vegetation and moisture-related spectral patterns across the Phagwara area, whereas the research farm maps focus on wheat-specific spectral responses within the selected field boundary. As the regional-scale maps may include mixed land-use classes, the research farm boundary was used to extract wheat-specific spectral information and minimize the influence of non-wheat pixels.

False color composite (FCC)

False Colour Composite (FCC) imagery proved effective in assessing vegetation vigour and temporal changes during the *Rabi* seasons of 2022–23 and 2023–24 in the Phagwara region (Fig. 3a and b). The FCCs were generated by assigning NIR, red, and green bands to the red, green, and blue channels, respectively,

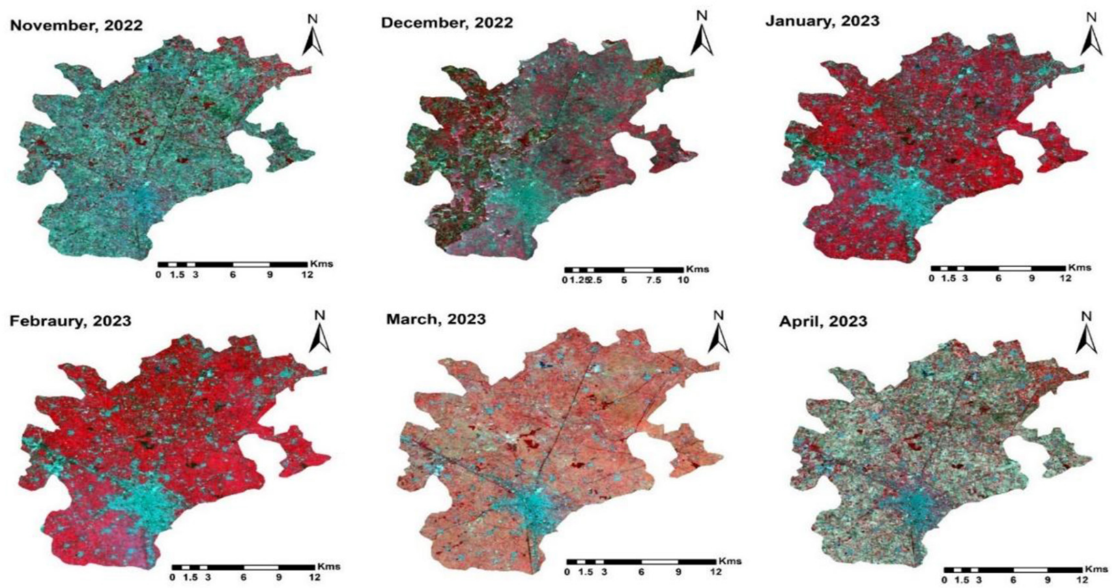

Fig. 3(a): FCC map for Phagwara region during the *rabi* season of 2022-23

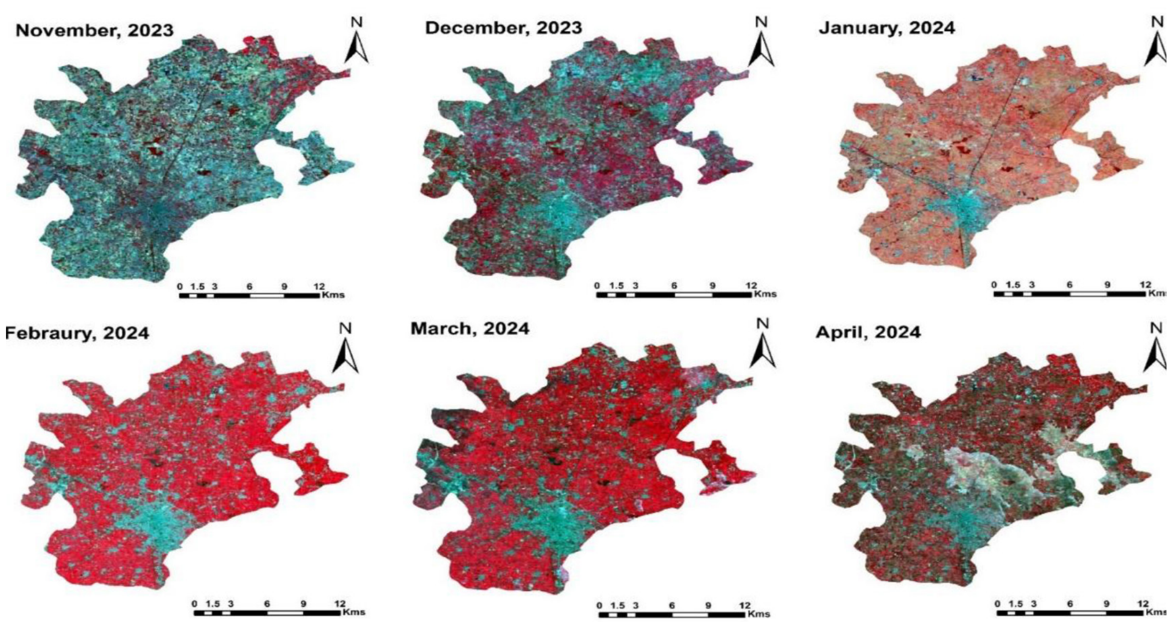

Fig. 3(b): FCC map for Phagwara region during the *rabi* season of 2023-24

which enhanced the visual differentiation between vegetation, built-up areas, and water bodies. Healthy vegetation appeared in varying shades of red, while blue and cyan tones represented fallow or built-up land. During November 2022, the red hues were faint, reflecting early crop establishment and limited vegetation cover. From December to February, an increase in bright red coloration indicated enhanced vegetation density and chlorophyll activity, corresponding to the active vegetative phase of wheat. In March, the red tones slightly diminished, suggesting crop maturation and a decline in NIR reflectance. By April, the predominance of cyan and yellow shades signified crop harvesting and reduced vegetative activity. A similar pattern was observed during 2023–24**.** November again showed weak red tones due to early sowing. The red intensity increased in December and February, indicating healthy canopy growth, while a lighter red in January was linked to lower temperatures that temporarily slowed photosynthesis and reduced chlorophyll concentration. As temperatures rose in February and March**,** red tones deepened, marking vigorous growth, followed by a decline in April as crops approached maturity. These seasonal colour variations align with earlier findings that vegetation reflectance in the NIR band is strongly influenced by plant physiological status and ambient temperature (Jensen, 2007; Campbell & Wynne, 2011; Lillesand *et al.,* 2015). Thus, FCC imagery effectively captured phenological transitions and moisture stress variations,

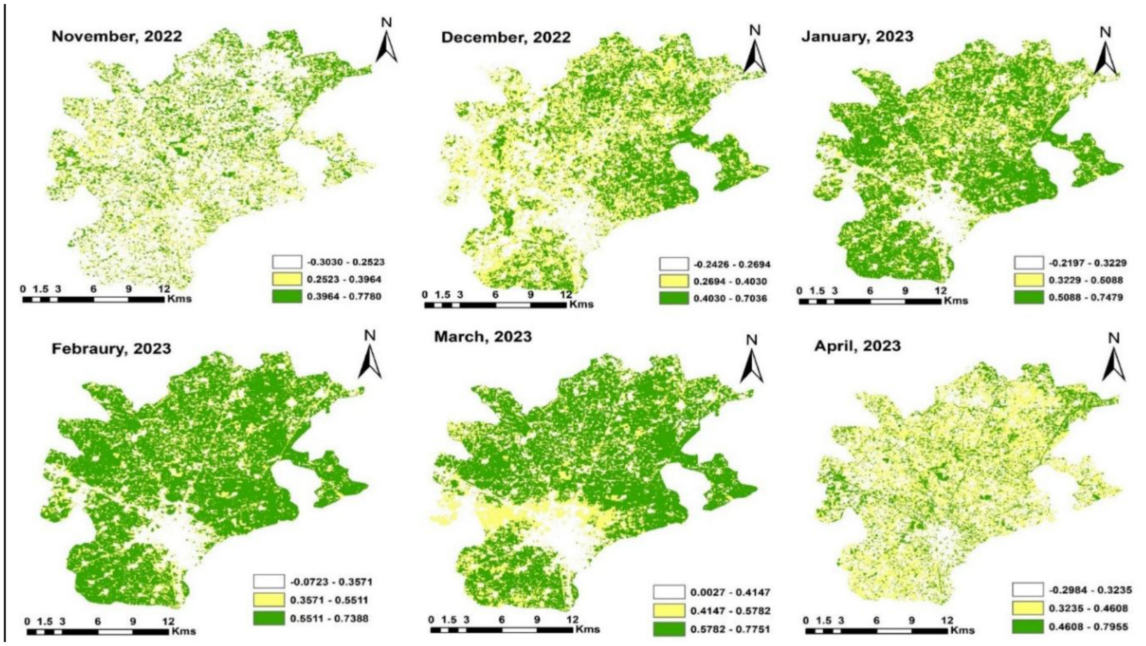

Fig. 4(a): NDVI map for Phagwara region during the *rabi* season of 2022-23

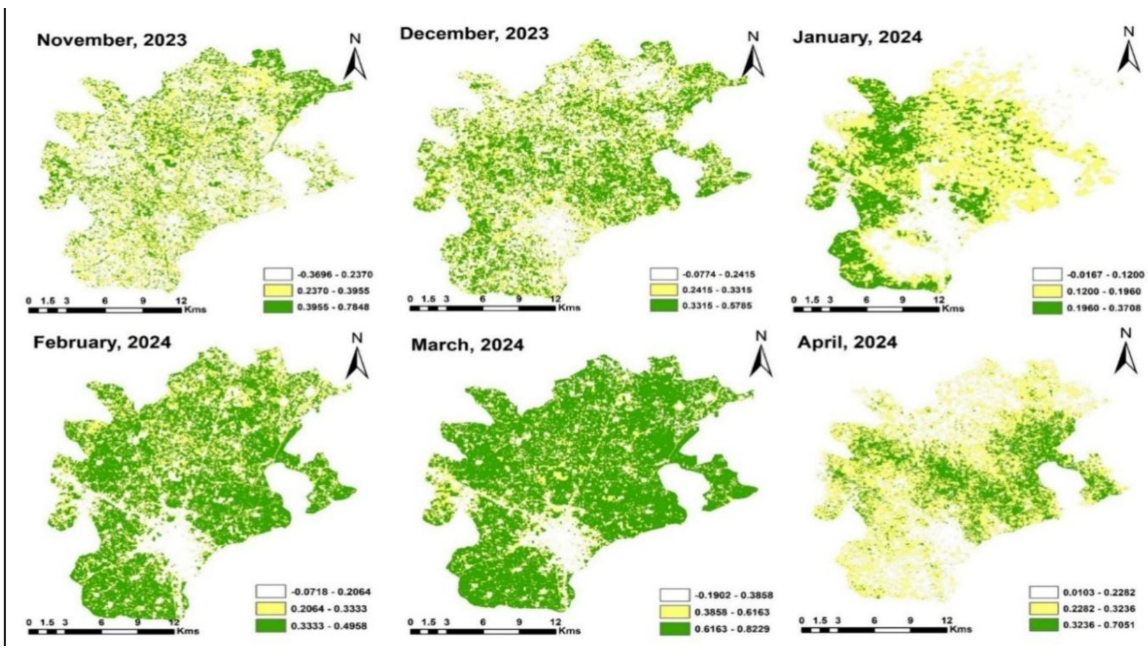

Fig. 4(b): NDVI map for Phagwara region during the *rabi* season of 2023-24

demonstrating its utility for monitoring crop development and vegetation health in wheat-growing areas.

Normalized difference vegetation index

The NDVI maps of the Phagwara region during the *rabi* seasons of 2022–23 and 2023–24 showed a clear seasonal pattern of wheat growth, with lower NDVI during crop establishment, higher NDVI during active vegetative/reproductive growth, and a decline toward maturity. During 2022–23, NDVI values ranged from –0.3030 to 0.7780 in November, indicating sparse vegetation and soil background influence after sowing. NDVI increased during December and January, with values ranging from –0.2426 to 0.7036 and –0.2197 to 0.7479, respectively, reflecting progressive canopy development. The highest vegetation vigour was observed during February and March, when NDVI ranged from –0.0723 to 0.7388 and 0.0027 to 0.7751, respectively, corresponding to active vegetative and reproductive growth stages. In April, although NDVI ranged from –0.2984 to 0.7955, the increased dominance of low to moderate NDVI classes indicated crop senescence, canopy drying, and maturity (Fig. 4a).

A similar pattern was observed during 2023–24 (Fig. 4b).

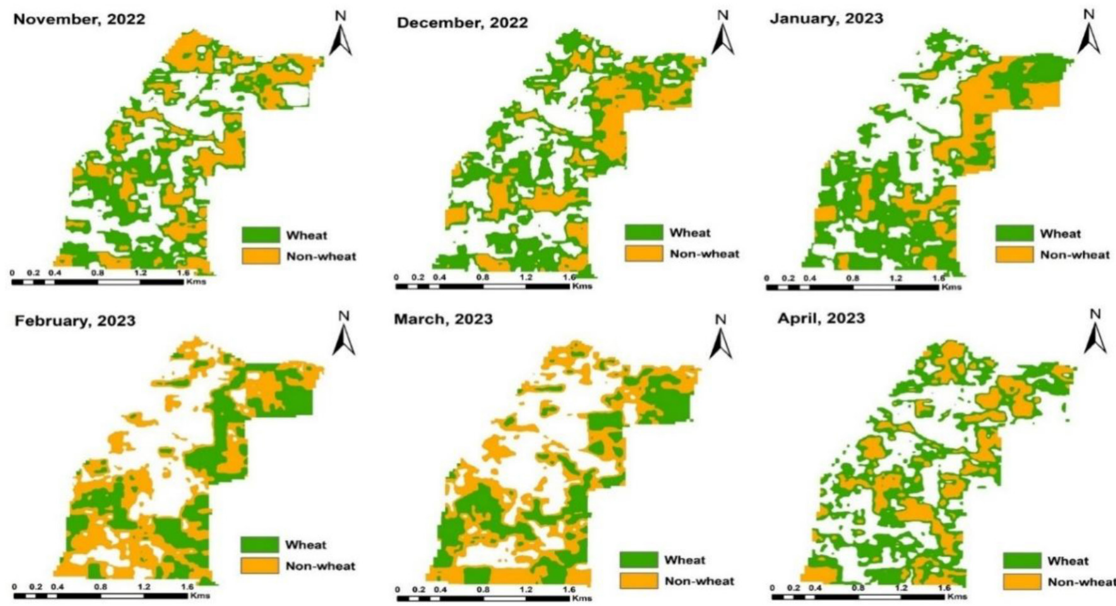

Fig. 5(a): NDVI map of the selected LPU Research Farm wheat field during the *rabi* season of 2022–23.

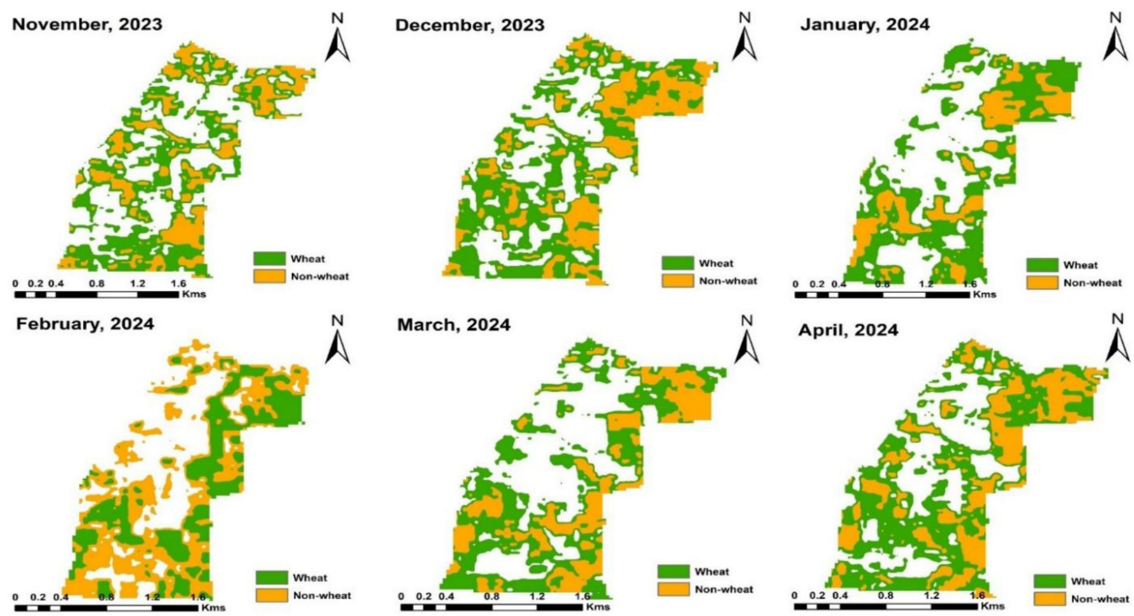

Fig. 5(b): NDVI map of the selected LPU Research Farm wheat field during the *rabi* season of 2023-24

NDVI values ranged from –0.3696 to 0.7848 in November and –0.0774 to 0.5785 in December, indicating early crop establishment and gradual canopy development. In January 2024, NDVI values declined comparatively, ranging from –0.0167 to 0.3708, which may be attributed to low winter temperature restricting canopy expansion and chlorophyll activity. NDVI increased again during February and March, with values ranging from –0.0718 to 0.4958 and –0.1902 to 0.8229, respectively, showing improved crop vigour and maximum canopy development during the peak growth period. In April 2024, NDVI ranged from 0.0103 to 0.7051, but the greater occurrence of low to moderate NDVI classes indicated senescence and maturity. Overall, both seasons followed the expected wheat growth trend, with NDVI increasing from early establishment to peak growth and declining toward maturity. Similar seasonal NDVI behaviour in wheat, with increasing values during vegetative growth and declining values during maturity, has been reported by Vermote *et al.,* (2016) and Huang *et al.,* (2022). The decline in NDVI during later stages is mainly associated with reduced chlorophyll content, lower near-infrared reflectance, and increased red reflectance due to senescence and canopy drying (Zhang *et al.,* 2003; Bhandari *et al.,* 2012).

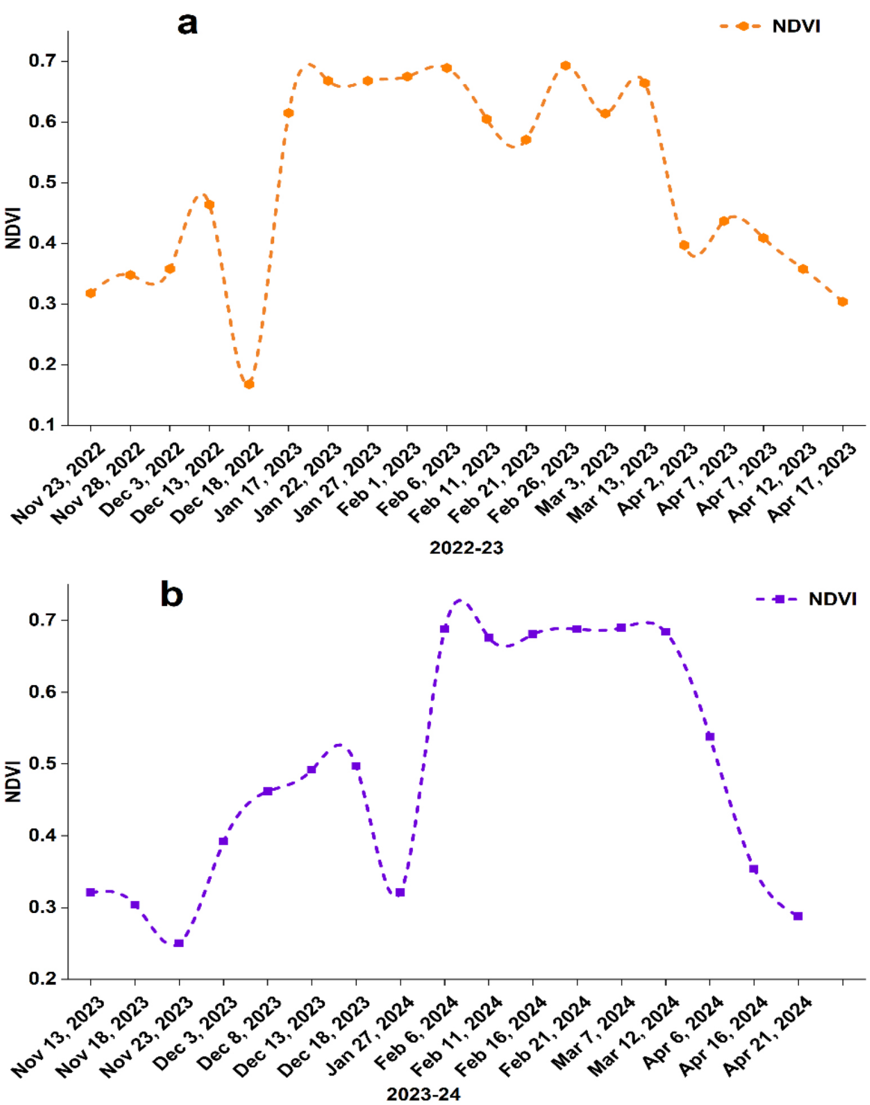

Fig. 6: Growth-stage-wise spectral reflectance pattern of wheat in the Phagwara region during the *Rabi* seasons of (a) 2022–23 and (b) 2023–24

NDVI-based wheat classification in the selected study area

The NDVI-based wheat and non-wheat classification maps of the selected study area during *rabi* 2022–23 and 2023–24 showed temporal variation in wheat distribution across different crop growth stages (Fig. 5a and b). During November in both seasons, wheat pixels were scattered because the crop was at the sowing/early establishment stage, with limited canopy cover and greater exposed soil background. In December and January, the proportion of wheat pixels increased, indicating progressive crop establishment, tillering, and canopy expansion. During February and March, wheat pixels became more prominent in the selected field boundary, corresponding to the active vegetative and reproductive growth phases, when crop vigour, leaf area, and canopy cover were higher. By April, the classification pattern became more mixed, reflecting crop maturity, senescence, canopy drying, and partial harvesting.

A broadly similar temporal pattern was observed in both years; however, some variation in wheat pixel distribution between 2022–23 and 2023–24 may be attributed to differences in crop growth, sowing pattern, temperature, rainfall, and field-level management. The seasonal increase in wheat pixels from early growth to peak vegetative/reproductive stages and their reduction or mixed distribution toward maturity is consistent with the expected NDVI response of wheat, where NDVI increases with canopy development and declines during senescence and harvesting (Vermote *et al.,* 2016; Huang *et al.,* 2022). The decline during later stages is mainly associated with reduced chlorophyll content, lower green biomass, and canopy drying (Zhang *et al.,* 2003; Bhandari *et al.,* 2012).

Regional and field-scale temporal NDVI dynamics of wheat

The temporal NDVI response showed a similar seasonal pattern in both the Phagwara region and the selected LPU Research Farm study area, with NDVI increasing from sowing/ early establishment to peak vegetative and reproductive stages,

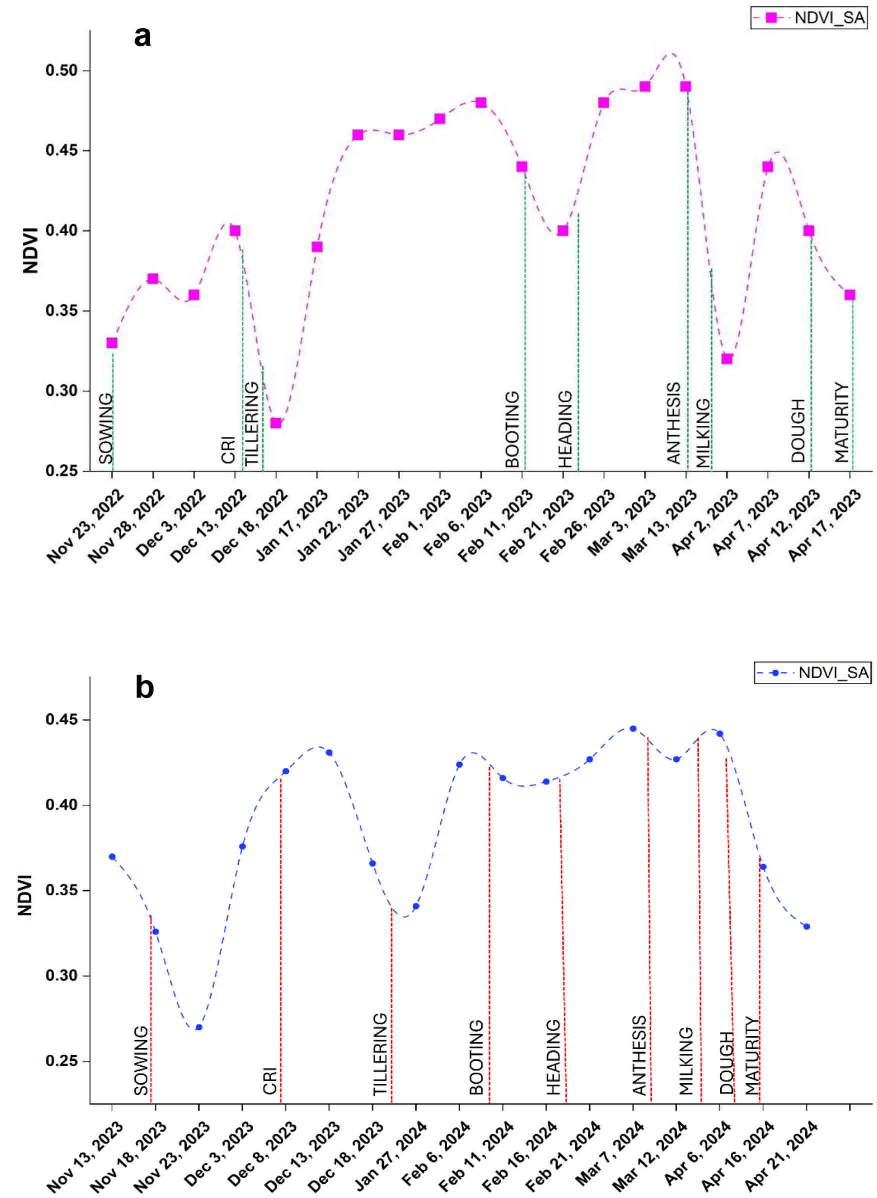

Fig. 7: Temporal variation in Landsat 8-derived NDVI of wheat within the selected LPU Research Farm boundary during the *Rabi* seasons of (a) 2022–23 and (b) 2023–24

followed by a decline toward maturity. However, the magnitude and fluctuations of NDVI differed between the two spatial scales. At the Phagwara regional scale, NDVI values showed a wider range, increasing from approximately 0.31–0.36 during early crop establishment to about 0.66–0.70 during the peak growth period in 2022–23. In 2023–24, NDVI similarly increased from around 0.25–0.37 during early growth to approximately 0.68–0.72 during February–March. The higher peak NDVI values at the regional scale indicate dense vegetation patches during the active wheat growth period; however, the greater fluctuations may be attributed to spatial heterogeneity, mixed land-use classes, variation in sowing dates, irrigation practices, crop density, and non-wheat vegetation within the broader Phagwara region (Fig. 6).

In contrast, the selected LPU Research Farm study area showed comparatively moderate NDVI values but a clearer field-level association with phenological stages. During 2022–23, NDVI increased from about 0.33 at sowing to approximately 0.48–0.51 during booting to anthesis, followed by a decline to around 0.36 toward maturity. During 2023–24, NDVI ranged from about 0.27–0.37 during early establishment and increased to approximately 0.42–0.45 during booting, heading, and anthesis, before declining toward maturity. The lower NDVI magnitude in the study area may be due to field-specific pixel averaging, boundary effects, soil background exposure, crop-stage variability, and the moderate spatial resolution of Landsat 8 imagery (Fig. 7).

Overall, both Phagwara and the study area followed the expected wheat growth trend, with NDVI increasing during canopy development and declining during senescence. The Phagwara-

Table 2: Stage-wise field observations used for interpretation of satellite-derived NDVI trends and moisture-related spectral response in wheat

Crop stage / DAS	Treatment	Plant height (cm)	LAI	RWC (%)	Interpretation for spectral indices
Vegetative stage / 60 DAS	T_1	46.6	2.71	87.2	Higher canopy growth, LAI, biomass and water status supported increasing NDVI and higher moisture-related spectral response
	T_2	36.9	2.27	74.2	Lower crop growth and water status indicated reduced canopy vigour
Reproductive phase / 90 DAS	T_1	91.0	4.51	84.2	Maximum canopy development and biomass supported peak NDVI response
	T_2	70.3	3.60	68.9	Reduced LAI, biomass and RWC indicated comparatively lower vegetation vigour
Grain filling/ 120 DAS	T_1	100.7	4.25	83.6	Maintained canopy and water status supported sustained vegetation activity
	T_2	77.7	3.35	66.6	Lower RWC and reduced canopy development supported drying and senescence-related spectral decline

scale response captured broader spatial variability in vegetation conditions, whereas the study-area response provided a more direct link with field-observed phenological stages. Therefore, the combined interpretation of regional and field-scale NDVI curves strengthens the assessment of wheat growth dynamics and supports the use of Landsat 8-derived NDVI for monitoring crop phenology.

Field-level interpretation of spectral indices using crop growth observations

To support the interpretation of satellite-derived spectral indices, selected field observations from contrasting irrigation treatments were used as ground reference. The recommended irrigation treatment (T_1) represented optimum crop growth, whereas the rainfed treatment (T_2) represented moisture-limited conditions. The stage-wise field observations supported the temporal NDVI pattern observed in the LPU study area. During the vegetative phase, T_1 showed higher plant height (46.6 cm), LAI (2.71) and RWC (87.2%) than T_2, where values were 36.9 cm, 2.27 and 74.2%, respectively. This corresponded with the increasing NDVI trend during early crop growth due to canopy expansion and biomass development. During the reproductive phase, the highest canopy vigour was observed under T_1, with plant height of 91.0 cm, LAI of 4.51 and RWC of 84.2%, compared with 70.3 cm, 3.60 and 68.9% under T_2. These values supported the peak NDVI response during active canopy development. At 120 DAS, T_1 maintained higher plant height (100.7 cm), LAI (4.25) and RWC (83.6%) than T_2, which showed lower values of 77.7 cm, 3.35 and 66.6%. This supported the gradual decline in NDVI during grain filling to early senescence, mainly due to reduced green canopy and canopy drying (Table 2).

Land surface water index

The Land Surface Water Index (LSWI), derived from NIR and SWIR reflectance, was used to assess moisture-related spectral variation during wheat growth. Since water strongly absorbs SWIR radiation, higher LSWI values generally indicate greater surface and canopy moisture, whereas lower values reflect comparatively drier conditions. During 2022–23, LSWI ranged from −0.350 to 0.807 in November, −0.611 to 0.941 in December, −0.331 to 0.787 in January, −0.744 to 0.674 in February, −0.071 to 0.618 in March, and −0.421 to 0.730 in April. During 2023–24, values ranged from −0.556 to 0.827, −0.380 to 0.652, −0.422 to 0.589, −0.407 to 0.747, −0.358 to 0.799, and −0.405 to 0.874 from November to April, respectively (Fig. 8 and 9). The wide variation in LSWI indicates spatial differences in crop cover, soil exposure, irrigation/rainfall influence, and surface moisture conditions across the study area. The observed LSWI pattern was also supported by meteorological conditions during the *rabi* seasons. Temperature ranged from 7.3 to 36.5 °C in 2022–23 and from 4.64 to 34.66 °C in 2023–24, while rainfall was 118.5 and 104.5 mm, respectively. Comparatively higher LSWI values during early and active growth stages may be attributed to cooler conditions, rainfall or irrigation inputs, and increasing canopy moisture. In contrast, lower LSWI values toward maturity were associated with rising temperature, reduced surface moisture, canopy drying, and senescence. Thus, LSWI effectively reflected the seasonal moisture-related variation associated with wheat growth and prevailing weather conditions in the study area. Previous studies have validated LSWI as a reliable indicator of water availability in both soil and vegetation (Chandrasekar *et al.,* 2010; Dangwal *et al.,* 2016), demonstrating strong correlation with observed water stress in wheat crops using multi-temporal Landsat imagery.

CONCLUSION

The study demonstrated the utility of multi-temporal Landsat 8-derived NDVI for assessing wheat vegetation dynamics and phenological progression in the Phagwara region during the *rabi* seasons of 2022–23 and 2023–24. NDVI showed a consistent seasonal pattern, with lower values during sowing and early establishment, increasing values during canopy expansion and peak vegetative–reproductive growth, and declining values during maturity due to senescence, reduced chlorophyll content, and canopy drying. The temporal NDVI profiles from the selected LPU Research Farm boundary corresponded with field-observed phenological stages, supporting the use of NDVI for regional and field-scale wheat growth monitoring. NDVI-based classification helped distinguish wheat and non-wheat pixels, while FCC imagery supported visual interpretation of vegetation and land-cover variability. LSWI provided supplementary information on moisture-related spectral variation; however, its interpretation remained

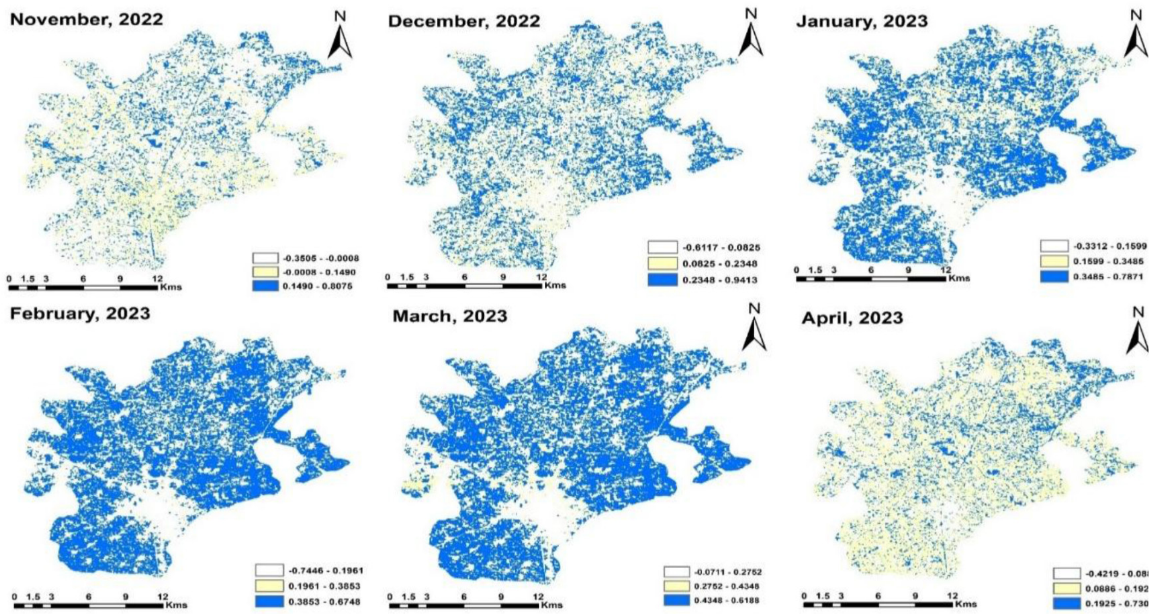

Fig. 8: LSWI-based moisture-related spectral variation in the Phagwara region during *Rabi* 2022–23

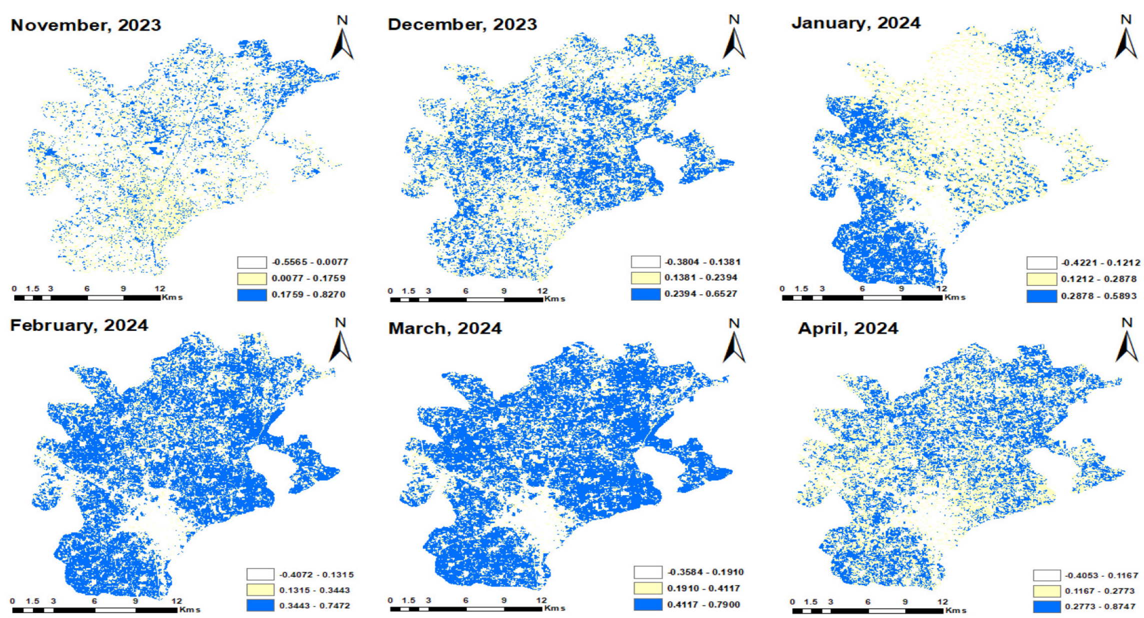

Fig. 9: LSWI-based moisture-related spectral variation in the Phagwara region during *Rabi* 2023–24

indicative due to the lack of stage-wise mean LSWI values and direct validation with field moisture measurements.

ACKNOWLEDGEMENT

The authors are thankful to the Department of Agronomy, School of Agriculture, Lovely Professional University for providing the opportunity to complete the research experiment.

Author's certificate: The manuscript or its part is not under consideration for publication elsewhere and the same has been approved by all co-authors.

Conflict of Interests: The authors declare that there is no conflict of interest regarding the publication of this article.

Funding: This research did not receive any specific funding.

Data Availability: The authors confirm that the data supporting our findings are available within the article.

Authors contribution: **Gurleen Kaur (GK), Vandna Chhabra (VC), and Vikas Sharma (VS):** Have contributed to the study conception and design. Material preparation and data collection along with the analysis was performed by GK. The manuscript was prepared by GK and edited by Sreethu S (SS) and VC.

Disclaimer: The contents, opinions, and views expressed in the research article published in the Journal of Agrometeorology are the views of the authors and do not necessarily reflect the views of the organisations they belong to.

Publisher's Note: The periodical remains neutral concerning jurisdictional claims in published maps and institutional affiliations.

REFERENCES

Barrs, H. D. & Weatherley, P. E. (1962). A re-examination of the relative turgidity technique for estimating water deficit in leaves. *Australian Journal of Biological Sciences*, 15*(*3), 413-428.

Bhandari, A. K., Kumar, A. & Singh, G. K. (2012). Feature extraction using Normalized Difference Vegetation Index (NDVI): A case study of Jabalpur city. *Procedia Technology*, 6, 612-621.

Campbell, J. B. & Wynne, R. H. (2011). *Introduction to remote sensing*. Guilford press.

Chandrasekar, K., Sesha Sai, M. V. R., Roy, P. S. & Dwevedi, R. S. (2010). Land Surface Water Index (LSWI) response to rainfall and NDVI using the MODIS Vegetation Index product. *International Journal of Remote Sensing, 31*(15), 3987-4005.

Dangwal, N., Patel, N. R., Kumari, M. & Saha, S. K. (2016). Monitoring of water stress in wheat using multispectral indices derived from Landsat-TM. *Geocarto International*, 31(6), 682-693.

Government of India. (2022). Agricultural statistics at a glance. Ministry of Agriculture, Department of Agriculture and Cooperation, Directorate of Economics and Statistics, Government of India.

Huang, X., Huang, J., Li, X., Shen, Q. & Chen, Z. (2022). Early mapping of winter wheat in Henan province of China using time series of Sentinel-2 data. *GIScience and Remote Sensing*, 59(1), 1534-1549.

Jensen, J. R. (2007). *Remote sensing of the environment: An earth resource perspective*. Pearson Education.

John, D. A., & Babu, G. R. (2021). Lessons from the aftermaths of green revolution on food system and health. *Frontiers in sustainable food systems, 5*:644559. https://doi.org/10.3389/fsufs.2021.644559.

Kaur, B., Sidhu, R. S., & Vatta, K. (2010). Optimal crop plans for sustainable water use in Punjab. *Agricultural Economics research review, 23*(2): 273-284.

Lillesand, T., Kiefer, R. W. & Chipman, J. (2015). *Remote sensing and image interpretation*. John Wiley & Sons.

Nageswara, R., Reddy, K. R. & Rao, V. (2005). Determination of vegetation indices for assessing crop health using remote sensing. *Journal of Remote Sensing and Earth Observation*, *10*(2), 123-130.

Radočaj, D., Šiljeg, A., Marinović, R., & Jurišić, M. (2023). State of major vegetation indices in precision agriculture studies indexed in web of science: A review. *Agriculture*, 13(3), 707.

Shi, X., Shi, W., Dai, N., & Wang, M. (2022). Optimal irrigation under the constraint of water resources for winter wheat in the north China plain. *Agriculture,* 12(12):2057. https://doi.org/10.3390/agriculture12122057.

Sidhu, J. K. & Chopra, M. (2022). An appraisal of legal framework for groundwater governance in Punjab. *Current World Environment,* 17:74–87. https://doi.org/10.12944/CWE.17.1.7.

Srivastava, S. K., Chand, R., Raju, S. S., Jain, R., Sachdeva, J., Singh, J., & Kaur, A. P. (2015). Unsustainable groundwater use in Punjab agriculture: insights from cost of cultivation survey. *Indian Journal of Agricultural Economics,* 70(3): 367-378. https://doi.org/10.22004/ag.econ.230215.

Tucker, C. J. (1979). Red and photographic infrared linear combinations for monitoring vegetation. *Remote Sensing of Environment, 8*(2), 127-150.

Vermote, E. F., Justice, C. O. & Bréon, F. M. (2016). Monitoring agriculture in India using MODIS NDVI time series. *Remote Sensing of Environment, 169*, 119-134.

Yang, Y., Zhu, J., Zhao, C., Liu, S., & Tong, X. (2011). The spatial continuity study of NDVI based on Kriging and BPNN algorithm. *Mathematical and Computer Modelling*, *54*(3-4), 1138-1144.

Zhang, X., Wang, M. & Liu, C. (2003). Monitoring rice crop conditions using Landsat NDVI. *Remote Sensing of Environment. 85*(3), 350-358.